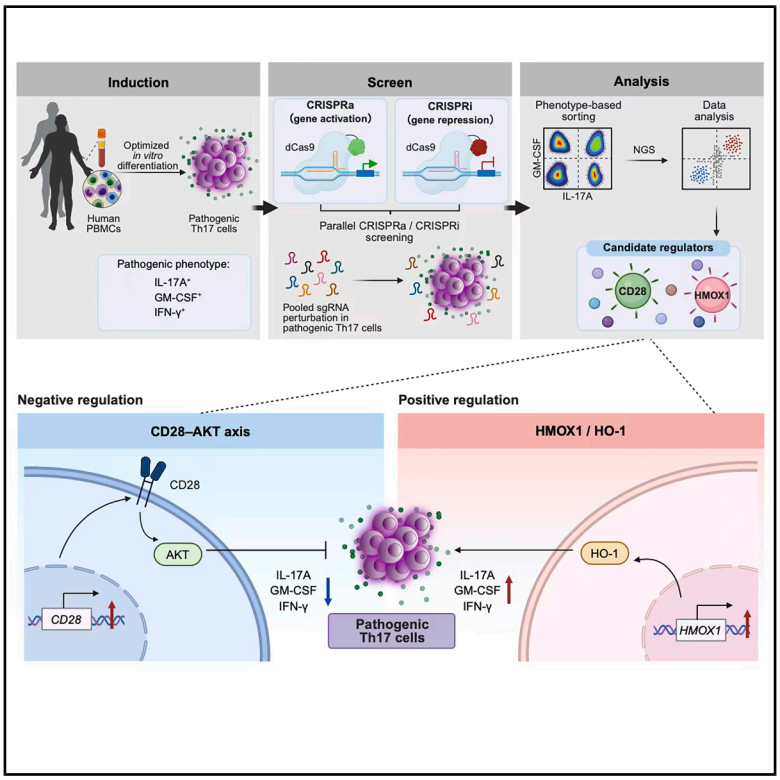
iScience

Article

Systematic CRISPR screens decode regulators of primary human pathogenic Th17 cell differentiation and activation

Graphical abstract



Highlights

- An optimized culture system enables human pathogenic Th17-like differentiation
- Parallel CRISPRa/i screens identify regulators of pathogenic Th17 cells
- CD28–AKT signaling negatively regulates pathogenic Th17 differentiation
- HMOX1 promotes pathogenic Th17 differentiation and activation *in vitro*

Authors

Yuan Wang, Zekun Yu, Lixin Wang, ..., Biao Zhou, Kecheng Li, Xuanming Yang

Correspondence

xuanmingyang@sjtu.edu.cn

In brief

Immunology; Genetics; Cell biology

Wang et al., 2026, iScience *29*, 118180
November 20, 2026 © 2026 The Author(s). Published by Elsevier Inc.
https://doi.org/10.1016/j.isci.2026.118180

CellPress

iScience

CellPress
OPEN ACCESS

Article

Systematic CRISPR screens decode regulators of primary human pathogenic Th17 cell differentiation and activation

Yuan Wang,[1,7] Zekun Yu,[1,7] Lixin Wang,[2] Junshi Zhang,[1] Wanting Wang,[1] Ban Luo,[1] Bochen Huang,[1] Fanmeng Zhang,[1] Lu Zhang,[3] Chenchen Shen,[4] Biao Zhou,[2] Kecheng Li,[2] and Xuanming Yang[1,5,6,8,*]

[1]Sheng Yushou Center of Cell Biology and Immunology, School of Life Sciences and Biotechnology, Shanghai Jiao Tong University, Shanghai 200240, China
[2]Angel Pharmaceuticals Co., Ltd., Jiaxing 314000, China
[3]Department of Oncology, Tongji Hospital, Tongji Medical College, Huazhong University of Science and Technology, Wuhan 430030, China
[4]Department of Mathematics and Statistics, Northeastern University at Qinhuangdao, Qinhuangdao 066004, China
[5]Department of Gynaecology and Obstetrics, Shanghai Pudong New Area People's Hospital, Shanghai 201299, China
[6]State Key Laboratory of Microbial Metabolism, Joint International Research Laboratory of Metabolic & Developmental Sciences, Shanghai Jiao Tong University, Shanghai 200240, China
[7]These authors contributed equally
[8]Lead contact
*Correspondence: xuanmingyang@sjtu.edu.cn
https://doi.org/10.1016/j.isci.2026.118180

SUMMARY

T-helper 17 (Th17) cells mediate host defense against bacterial and fungal pathogens at mucosal and skin interfaces. However, they are also involved in the pathogenesis of diverse autoimmune and inflammatory diseases. To accelerate candidate discovery in the pathogenic Th17 pathway, we have customized druggable CRISPR activation (CRISPRa) and interference (CRISPRi) sgRNA libraries. With an optimized Th17 differentiation protocol, we performed customized CRISPRa and CRISPRi screens in human peripheral blood mononuclear cells (PBMCs) to identify potential regulators controlling the function of pathogenic Th17 cells. Coupled with next-generation sequencing, our screens identified previously reported and undiscovered genes involved in pathogenic Th17 cell differentiation and activation. Among them, the regulatory roles of heme oxygenase 1 and CD28 were verified by sgRNA-based and small-molecule inhibitor-based functional experiments *in vitro*. Our study provided a useful resource for mapping key genes of pathogenic Th17 cell function and potential immunotherapy targets for treating Th17-related immune disorders.

INTRODUCTION

$CD4^+$ T cells are critical for the generation, maintenance, and regulation of immune responses against non-self and self-antigens.[1–3] Several subsets of $CD4^+$ T cells have been identified based on their distinct lineage-defining transcription factors and major effector cytokines, such as Th1, Th2, Th17, and Treg, etc.[2] Among them, Th17 cells were named for their specific ability to produce IL-17 family cytokines.[4,5] The retinoic acid receptor-related orphan receptor-γt (RORγt) is the master transcription factor for Th17 differentiation, and Th17 cell development is severely impaired in RORγt KO mice.[6]

Th17 cells are critical for host defense against bacterial and fungal pathogens at mucosal and skin interfaces.[7–9] Different from Th1 and Th2 cells, Th17 cells have a close interaction with non-immune epithelial cells in the gut. Th17 cells secrete high levels of IL-17A, IL-17F, and IL-22.[10,11] These cytokines can act on epithelium in the gut to induce the expression of tight junction proteins and antimicrobial peptides, which are important for mucosal barrier integrity and defense function. However, Th17 cells are also involved in the pathogenesis of various autoimmune and inflammatory diseases. Anti-IL-17 pathway antibodies are effective in the treatment of some inflammatory conditions, including plaque psoriasis, psoriatic arthritis, and ankylosing spondylitis.[12–16] Analysis of Th17 cells under disease conditions has revealed the existence of a pathogenic Th17 subtype that differs from regular Th17 cells under physiological conditions. These pathogenic Th17 cells produce high amounts of GM-CSF and/or IFN-γ.[17,18] Both pathogenic and non-pathogenic Th17 cells produce IL-17. Pathogenic Th17 cells additionally express proinflammatory genes including *Csf2*, *Ifng*, and *Il23r*. It is reported that GM-CSF (*Csf2* coding protein) is the primary inducer of inflammation in some autoimmune disease models.[19–22] Dissection of the differentiation and activation

This is an open access article under the CC BY license (http://creativecommons.org/licenses/by/4.0/).

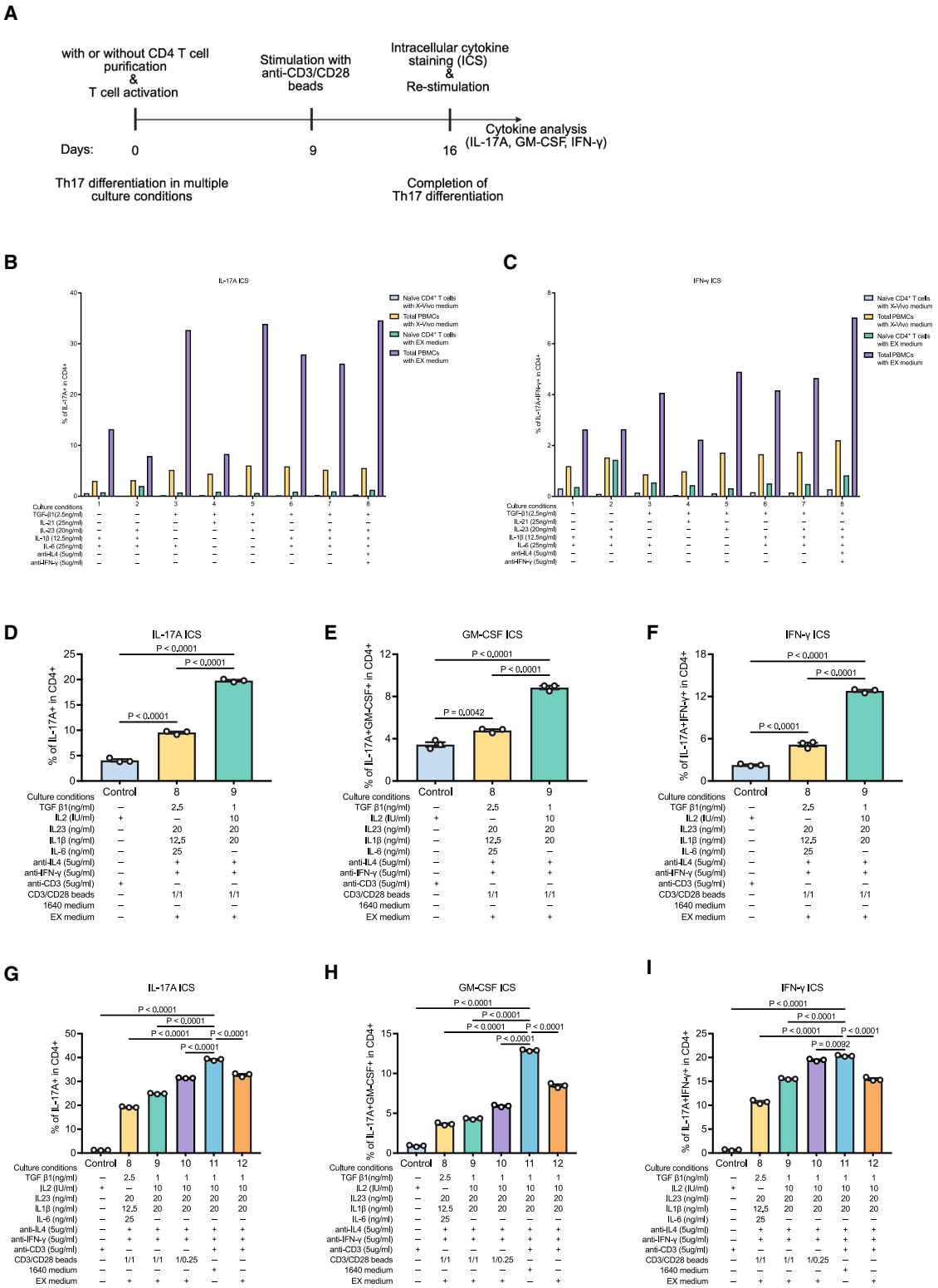


Figure 1. Optimization of differentiation conditions for human pathogenic Th17 cells *in vitro*

(A) Scheme of differentiation protocol for pathogenic Th17 cells.

(B and C) FACS analysis for IL-17A and IFN-γ production in Th17 cells under multiple differentiation conditions.

(legend continued on next page)

driver genes of pathogenic Th17 cells is critical for developing therapeutics in Th17-related autoimmune or inflammatory diseases.

In vitro polarization is a useful model to investigate key pathways involved in Th17 differentiation. IL-6 and TGF-β drive naive mouse $CD4^+$ T helper cells to differentiate into Th17 cells that produce IL-17 but little or no proinflammatory cytokines, while the combination of IL-6, IL-1β, and IL-23 or IL-6, TGF-β, and IL-23 promotes the development of pathogenic Th17 cells producing significant proinflammatory cytokines,[17,23] and can further induce autoimmune disease after adoptive transfer. These *in vitro* polarization conditions provide useful hints for discovering the key modulators of pathogenic Th17 differentiation. However, further extension to larger or systemic studies is hampered by inherent technical challenges. CRISPR-Cas9-based genetic approaches are useful tools for systematically uncovering the components of regulatory networks. Genome-wide CRISPR knockout screens have been used for discovery of drug-resistant genes in cancer cells, exhaustion-regulatory genes in T cells, and IFN-γ-producing regulatory genes in T cells, etc.[24–27] Beyond conventional knockout screens, CRISPR activation (CRISPRa) for gain-of-function and CRISPR interference (CRISPRi) screens for loss-of-function have been recently developed. Unlike complete gene ablation, CRISPRa and CRISPRi provide a more physiological, regulatable degree of gene expression, with nuanced approaches that mimic the therapeutic effects of small-molecule drugs.[27–29]

In this study, we optimized the *in vitro* differentiation method for human pathogenic Th17 cells and the Th17 cell activation method for efficient large-scale sgRNA library screening. We established two customized CRISPRa and CRISPRi sgRNA libraries covering 3,222 druggable targets. Using both CRISPRa and CRISPRi screens, we have identified a set of genes involved in the differentiation and activation of pathogenic Th17 cells and verified their phenotypes through genetic perturbation and pharmacological inhibition *in vitro*. In summary, we developed a platform for pooled CRISPRa and CRISPRi screens in human Th17 cells, which is useful for uncovering potential therapeutic targets of pathogenic Th17-related diseases.

RESULTS

Successful differentiation of pathogenic Th17 cells *in vitro*

While murine Th17 differentiation is well-established, the robust induction of human pathogenic Th17 cells *in vitro* remains a significant challenge. To investigate the regulatory mechanisms governing these cells, we first sought to develop a highly efficient and reproducible pathogenic Th17-like cell differentiation protocol using human peripheral blood mononuclear cells (PBMCs), focusing on the production of inflammatory cytokines GM-CSF and IFN-γ. An initial screen of eight culture conditions was designed, incorporating key Th17-polarizing cytokines (TGF-β1, IL-6, IL-1β, and IL-23) in either X-VIVO 15 or UniEx media (Figure 1A and Table S1). Consistent with its known role in Th17 specification, the inclusion of TGF-β1 enhanced $IL\text{-}17A^+$ cell induction (condition 2 vs. 7; Figures 1B and S1). Furthermore, the addition of neutralizing antibodies against IFN-γ and IL-4 (condition 7 vs. 8) further increased differentiation efficiency, likely by preventing lineage diversion toward Th1 and Th2 phenotypes (Figures 1B and 1C). Although murine studies suggest that TGF-β3 induces a more potent pathogenic phenotype than TGF-β1, we observed that TGF-β3-supplemented conditions yielded comparable $IL\text{-}17A^+$ frequencies but lower percentages of $IL\text{-}17A^+GM\text{-}CSF^+$ and $IL\text{-}17A^+IFN\text{-}\gamma^+$ (pathogenic) subsets (condition 14 vs. 15; Figures S2A–S2C). Notably, UniEx medium and the use of total PBMCs resulted in superior differentiation compared with X-VIVO 15 and purified naive $CD4^+$ T cells, respectively. The enhanced yields from total PBMCs suggest that auxiliary signals from other immune cell subsets facilitate Th17 polarization; consequently, total PBMCs were utilized for all subsequent optimizations.

We then benchmarked our top-performing condition (condition 8) against one protocol from the Littman group (condition 9),[30] utilizing similar combinations of TGF-β1, IL-1β, and IL-23 (Figures 1D–1F, condition 8 vs. 9; Figures S2D–S2F). While both protocols induced appreciable frequencies of $IL\text{-}17A^+$, $IL\text{-}17A^+GM\text{-}CSF^+$, and $IL\text{-}17A^+IFN\text{-}\gamma^+$ cells (Figures 1D–1F), condition 9 yielded a higher absolute T cell count, potentially due to low-dose IL-2 supplementation, and was therefore selected as the scaffold for further refinement.

To further optimize pathogenic Th17 induction, we modulated T cell receptor (TCR) activation intensity, as low-strength signals have been reported to favor Th17 differentiation.[31,32] Reducing the ratio of cells to anti-CD3/CD28 beads from 1:1 (high intensity) to 1:0.25 and 0.125 (low intensity) significantly increased the proportions of total $IL\text{-}17A^+$ and pathogenic $CD4^+$ $IL\text{-}17A^+GM\text{-}CSF^+$ and $IL\text{-}17A^+IFN\text{-}\gamma^+$ T cells (Figures 1G–1I, condition 9 vs. 10; Figures S2G–S2I, condition 10 vs. 13). Given that CD28 co-stimulation can negatively regulate Th17-related transcriptional programs,[31] we tested conditions lacking CD28 signaling (condition 12). This condition promoted pathogenic Th17 cell differentiation more effectively than or comparably to initial bead-based co-stimulation (Figures 1G–1I, condition 12 vs. 9, Figures S3A–S3C). Interestingly, media-specific effects were more pronounced under these conditions: RPMI 1640 complete medium (condition 11) outperformed UniEx (condition 12) in inducing the pathogenic phenotype under CD3-only condition (Figures 1G–1I and S3A–S3C). The superiority of condition 11—characterized by the absence of CD28 co-stimulation and RPMI 1640 medium—was consistently validated across multiple donors (Figures S3D–S3I). The representative flow cytometry plots of $IL\text{-}17A^+$, $IL\text{-}17A^+GM\text{-}CSF^+$, and $IL\text{-}17A^+IFN\text{-}\gamma^+$ cells under conditions 8–12 are shown in Figures S4A–S4F.

(D–F) FACS analysis for IL-17A, GM-CSF, and IFN-γ production in Th17 cells in TGF-β1, IL-1β, and IL-23-centered differentiation conditions ($n = 3$). See also Figures S2D–S2F.

(G–I) FACS analysis for IL-17A, GM-CSF, and IFN-γ production in Th17 cells in weak TCR stimulation and co-stimulation-less differentiation conditions ($n = 3$). See also Figures S3A–S3I. Data are presented as means ± SEM with statistical significance determined by ANOVA. The normality of data was confirmed by the Shapiro-Wilk test. Statistical significance was indicated by $^*p < 0.05$, $^{**}p < 0.01$, and $^{***}p < 0.001$.

To interrogate the lineage commitment of T cells differentiated *in vitro*, we quantified the expression of AhR and RORγt (Th17), T-bet (Th1), and FOXP3 (Treg) in $CD4^+$ T cells by flow cytometry. The results showed that condition 11 yielded higher expression levels of AhR and RORγt, while showing lower expression levels of T-bet and FOXP3 in $CD4^+$ T cells (Figures S5A–S5E). This transcription factor profile indicated that condition 11 preferentially induced a Th17-enriched phenotype while limiting deviation toward Th1 and Tregs.

In summary, we have established an optimized protocol (condition 11) that robustly generates human Th17 cells with a pathogenic-like phenotype, which focuses on the induction of the inflammatory cytokines GM-CSF and IFN-γ, providing a high-fidelity platform for studying their regulatory biology and functional roles in inflammatory disease. Referring to the results above, condition 11 was adopted for all subsequent experiments *in vitro*.

Establishment of a sorting-based pathogenic Th17 enrichment method and construction of customized druggable CRISPRa/i sgRNA libraries

To facilitate the identification of regulatory mechanisms underlying pathogenic Th17 ($CD4^+IL\text{-}17A^+GM\text{-}CSF^+$) cell differentiation and function, we first developed an optimized enrichment method based on flow cytometric sorting. Traditional approaches for isolating pathogenic Th17 cells rely on sequential surface markers and intracellular cytokine staining, which involve multiple wash and centrifugation steps that significantly compromise cell yield. To improve recovery, we optimized a one-step staining protocol by employing a fixation-compatible anti-CD4 antibody, thereby reducing handling-induced cell loss while maintaining staining fidelity (Figure S6; see STAR Methods for details). Building on this optimized enrichment strategy, we constructed customized CRISPRa and CRISPRi sgRNA libraries for functional screening in pathogenic Th17 cells, which survived after drug selection (Figure 2A). While T cells are differentiated into a pathogenic Th17 state *in vitro*, they remain in a relatively quiescent steady state once differentiation is complete. Restimulation via TCR signaling is biologically necessary to trigger the activation required for producing the functional effector cytokines IL-17A, GM-CSF, and IFN-γ, which serve as our primary screening readouts. CRISPRi screens enable the identification of essential regulatory pathways through transcriptional repression of gene expression, whereas CRISPRa (CRISPR activation) screens uncover limiting factors by upregulating gene transcription during specific biological states[33] (Figure S7). To increase the translational relevance of our screen, we focused on a curated subset of druggable genes and excluded essential genes that could confound downstream therapeutic targeting (Data S1 and S2). The druggable gene library focuses on actionable therapeutic targets. We selected genes within pathways accessible via small molecules or antibodies (such as ion channels, kinases, and GPCRs) while intentionally filtering out essential genes required for basic physiological function or "vital life". This facilitates convenient drug delivery and universal applicability in subsequent clinical translation. We adapted sgRNA designs from Sanson et al. Calabrese and Dolcetto whole-genome libraries to target our selected subset of druggable genes for CRISPRa and CRISPRi, respectively.[33] Each gene in the sgRNA libraries was targeted by six unique sgRNAs, resulting in >95% coverage across all selected targets. The optimized pathogenic Th17 enrichment protocol and the customized druggable CRISPRa/i sgRNA libraries provide robust and scalable tools for dissecting the molecular regulation of Th17 pathogenicity and identifying candidate therapeutic targets (Figure 2B).

CRISPRi and CRISPRa screen combination reveals critical genes/pathways of pathogenic Th17 differentiation

To determine critical genes and pathways of pathogenic Th17 differentiation systematically, we conducted CRISPRi and CRISPRa screens in parallel and sorted the Th17 population based on IL-17A and GM-CSF secretion profiles, yielding four distinct *in vitro*-differentiated, CRISPR-engineered $CD4^+$ T cell populations: $IL\text{-}17A^+GM\text{-}CSF^+$, $IL\text{-}17A^-GM\text{-}CSF^+$, $IL\text{-}17A^+GM\text{-}CSF^-$, and $IL\text{-}17A^-GM\text{-}CSF^-$. The inserted sgRNA cassettes in these populations were amplified and then underwent next-generation sequencing targeting the sgRNA fragments specifically. The quality of the data was estimated before analysis. The Q30 score, which represents a sequencing error rate of 1 in 1,000 bases, was above 90% for all the sequencing data, indicating high data quality. We employed two analytical comparisons to identify candidate genes regulating pathogenic Th17 cells: $IL\text{-}17A^+GM\text{-}CSF^+$ versus $IL\text{-}17A^-GM\text{-}CSF^-$, and $IL\text{-}17A^+GM\text{-}CSF^+$ versus $IL\text{-}17A^+GM\text{-}CSF^-$. The first comparison identifies factors influencing the co-production of both IL-17A and GM-CSF, while the second reveals factors specifically affecting GM-CSF production.

We first compared the pathogenic $IL\text{-}17A^+GM\text{-}CSF^+$ Th17 cells and the $IL\text{-}17A^-GM\text{-}CSF^-$ cells to calculate the log2-fold change (LFC) of each sgRNA-targeted gene by volcano plot analysis in T2, T4, and T5 donors (Figures 3A–3D). This analysis was based on sequencing of sgRNA abundances, as they manipulate the upregulation or downregulation of downstream genes, thereby reflecting differences in gene expression. Then, we combined data from different donors to identify shared mechanisms (Figures 3E and 3F). Many genes of interest are identified through these analyses, such as *GZMA*, *HMOX1*, *MMP3*, and *ADAM18*. To gain insights into the functional pathways enriched across CRISPRi and CRISPRa screens, we performed an investigation within the Kyoto Encyclopedia of Genes and Genomes (KEGG) and Gene Ontology (GO) libraries. After aggregating all the data, we determined that both CRISPRi and CRISPRa regulators of pathogenic Th17 differentiation were highly related to cytokine-cytokine receptor interaction, MAPK signaling pathway, JAK-STAT signaling pathway, and Toll-like receptor signaling pathway (Figure 3G). Most of them were related to protein phosphorylation, cell surface receptor signaling, and regulation of response to stimulus, which demonstrated significant roles of these genes/pathways in pathogenic Th17 cell differentiation (Figure 3H). Similarly, we conducted a comparison of $IL\text{-}17A^+GM\text{-}CSF^+$ Th17 cells and the $IL\text{-}17A^+GM\text{-}CSF^-$ cells. We identified some interesting genes such as *GZMB*, *MMP14*, *IL4*, *ADAM17*, *ITGA11*, and *NOTCH1* by LFC analysis (Figures 4A–4F). Although this comparison

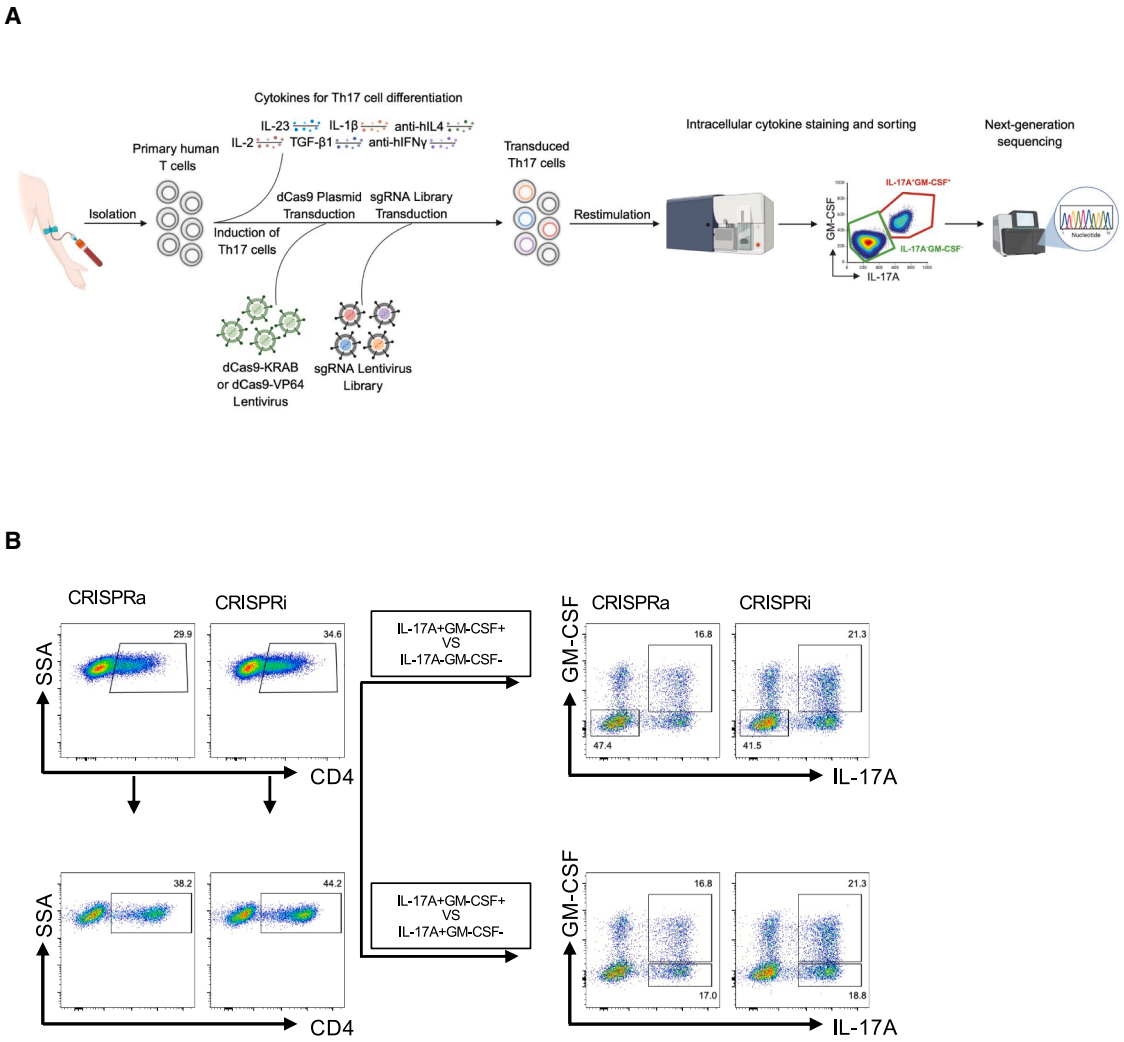


Figure 2. Establishment of a sorting-based pathogenic Th17 enrichment method and construction of customized druggable CRISPRa/i sgRNA libraries

(A) Schematic of CRISPRa/i screens for induced Th17 differentiation. Total PBMCs were differentiated in condition 11, transduced with CRISPRa or CRISPRi lentivirus, and cultured for about 10–13 days. After restimulation with PMA and ionomycin, cells were stained for intracellular IL-17A and GM-CSF, and IL-17A^{+}GM-CSF^{+}, IL-17A^{+}GM-CSF^{-}, IL-17A^{-}GM-CSF^{+}, and IL-17A^{-}GM-CSF^{-} populations were sorted. Integrated sgRNA cassettes were PCR-amplified and sequenced by NGS.

(B) Representative sorting data in CRISPRa- and CRISPRi-engineered Th17 cells.

focused on GM-CSF expression in IL-17A^{+} population, we observed very similar KEGG and GO enrichment patterns (Figures 4G and 4H), suggesting shared mechanisms between regulating GM-CSF and co-regulating GM-CSF and IL-17A in pathogenic Th17 cells.

We next completed the candidate gene determination for functional verification across CRISPRa and CRISPRi screens for pathogenic Th17 differentiation. We adhered to the following two principles when screening candidate genes: (i) the alterations of the gene are consistent within the CRISPRi or CRISPRa screens, while remaining opposite between them to the greatest extent possible; (ii) candidates were prioritized using a predefined false discovery rate (FDR) threshold of 0.2 for multiple-testing adjustment. After extensive screening, we identified several candidate genes potentially involved in the regulation of pathogenic Th17 cell differentiation (Figures 3 and 4). Among these, two genes—*CD28* and *HMOX1*—emerged as particularly noteworthy. CD28, a well-characterized co-stimulatory receptor, is critical for T cell activation, survival, proliferation, and cytokine production.[34] It has a lower FDR value, indicating higher confidence in the difference. *HMOX1*, encoding heme oxygenase 1, plays a central role in heme catabolism and has been previously implicated in modulating the balance between Th17 and Treg cells in murine models.[35] The alterations of *HMOX1* were identified in different experiments, showing consistent enrichment across screens (Figures 3B and 3E). Together, our CRISPRa and CRISPRi screening system effectively identified potential key regulators of pathogenic Th17 differentiation and function.

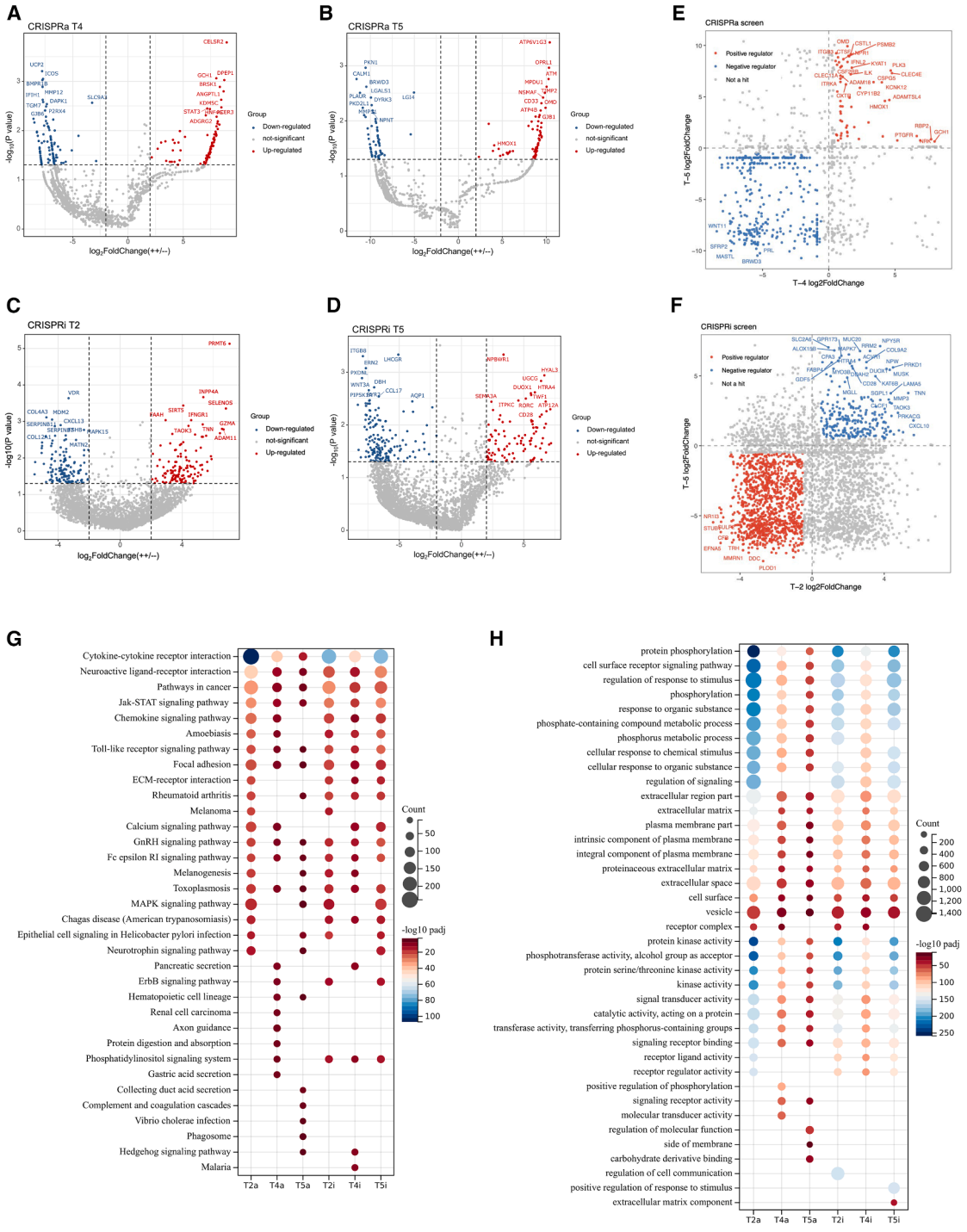


Figure 3. CRISPRi and CRISPRa screens of pathogenic Th17 cells comparing IL-17A^{+}GM-CSF^{+}and IL-17A^{-}GM-CSF^{-} populations

(A–D) Differential sgRNA expression volcano plot of CRISPRa and CRISPRi screens from different donor-derived PBMCs. T2, T4, and T5 represented independent experimental replicates. P value for the screen analyses were obtained using MAGeCK (see STAR Methods).

(E and F) Scatterplots of median sgRNA log2-fold change for each sgRNA-targeted gene, comparing screens in two donors.

(G and H) KEGG and GO enrichment analysis of CRISPRa and CRISPRi screens from all donors. Padj denotes the adjusted *p* value and color present -log10(padj).

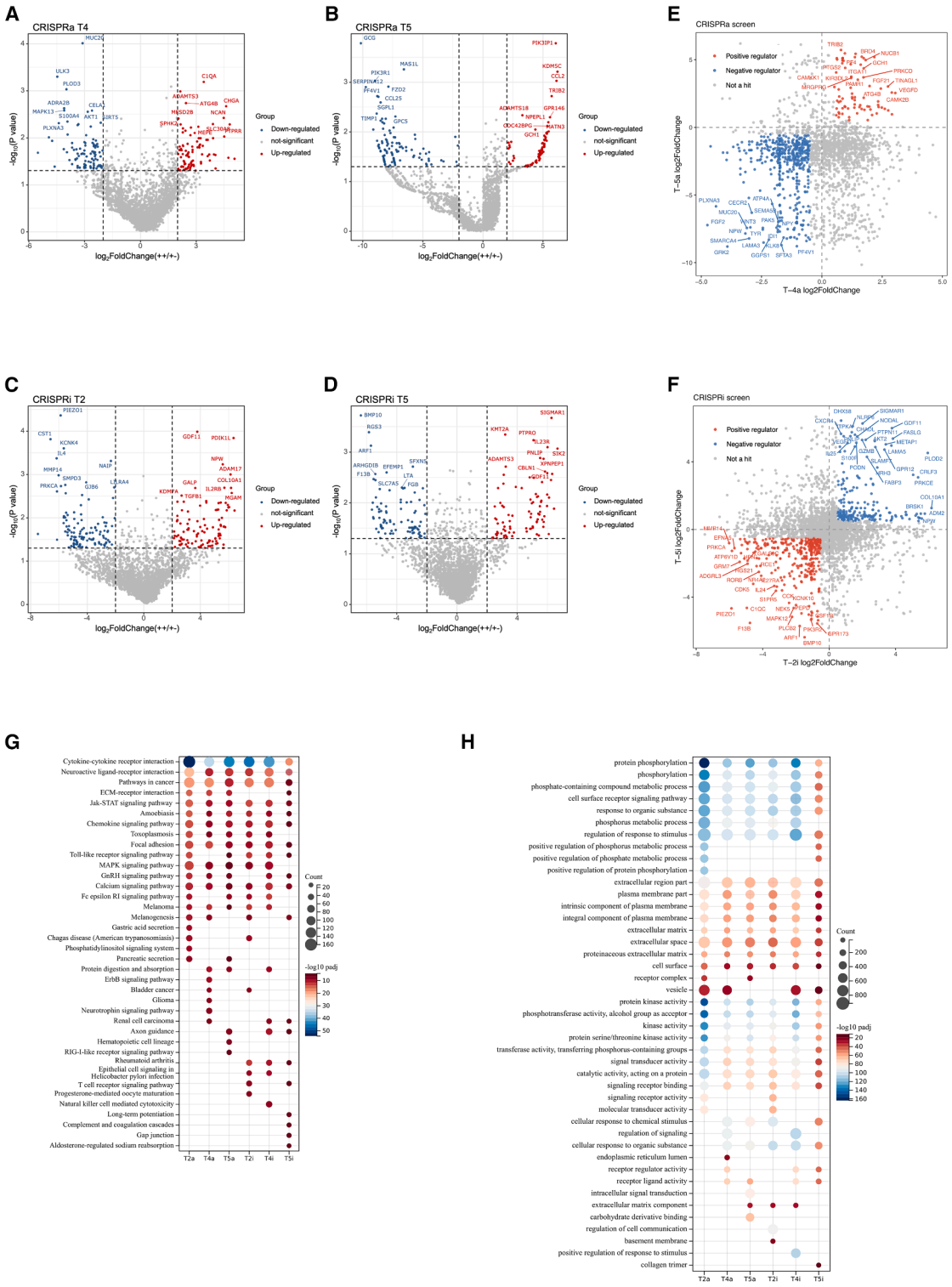


Figure 4. CRISPRi and CRISPRa screens of pathogenic Th17 cells comparing IL-17A$^+$GM-CSF$^+$, and IL-17A$^+$GM-CSF$^-$ populations

(A–D) Differential sgRNA expression volcano plot of CRISPRa and CRISPRi screens from different donor-derived PBMCs. P value for the screen analyses were obtained using MAGeCK (see STAR Methods).

(E and F) Scatterplots of median sgRNA log2-fold change for each sgRNA-targeted gene, comparing screens in two donors.

(G and H) KEGG and GO enrichment analysis of CRISPRa and CRISPRi screens from all donors. Padj denotes the adjusted *p* value and color represent -log10(padj).

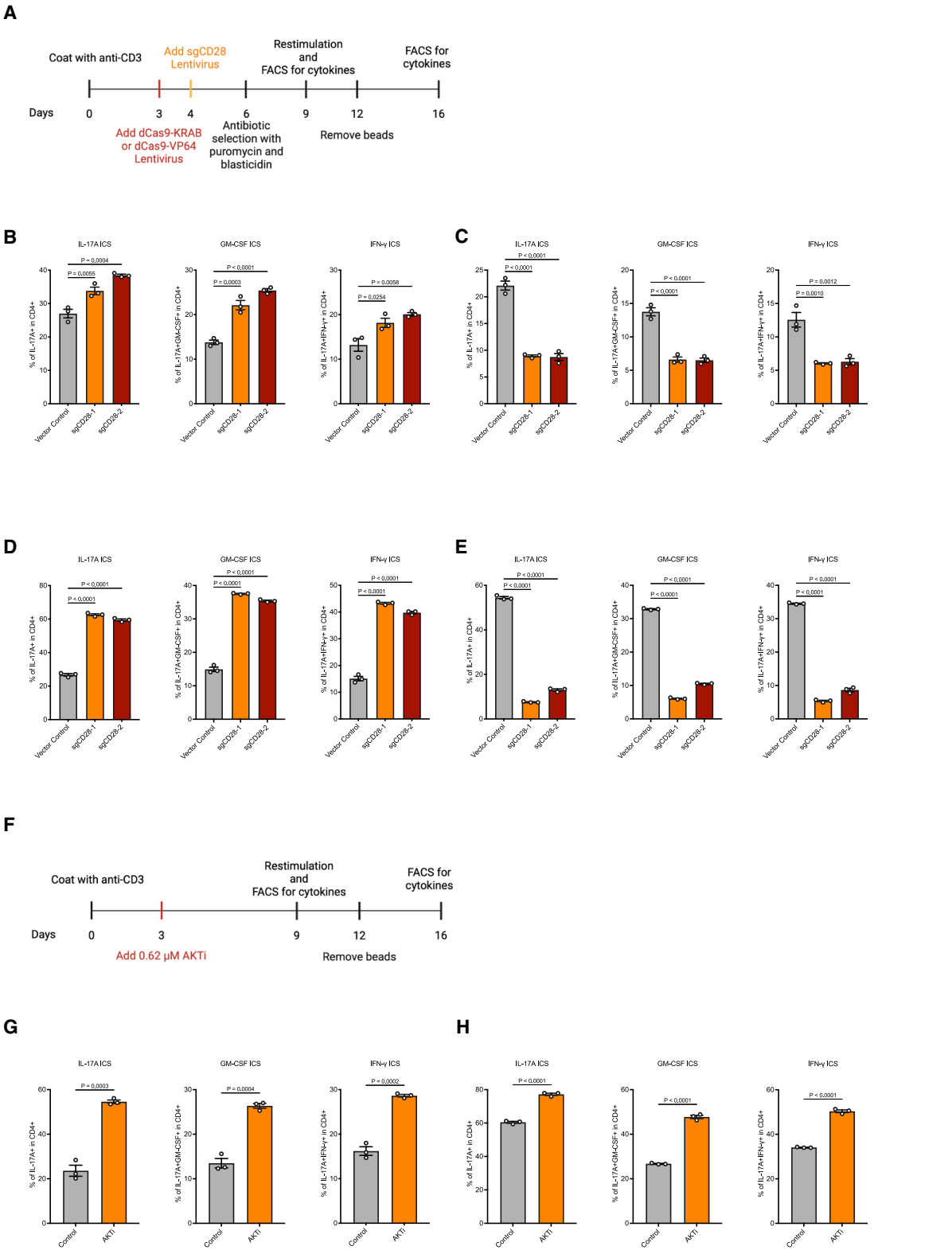


Figure 5. CD28-AKT signaling negatively regulates pathogenic Th17 differentiation

(A) Schematic diagram of Th17 cells treated with CRISPRa/i system targeting *CD28*.

(B and C) Flow cytometry analysis of IL-17A$^+$, IL-17A$^+$GM-CSF$^+$, and IL-17A$^+$IFN-γ$^+$ cells of the control and CRISPRi-CD28 sgRNA transduced Th17 cells (B) and CRISPRa-CD28 sgRNA-transduced Th17 cells (C) on day 9 after Th17 cell differentiation (n = 3).

(legend continued on next page)

CD28 and HMOX1 represent distinct pathways, co-stimulatory and metabolic, that warrant further investigation in functional validation studies.

CD28-AKT signaling negatively regulates pathogenic Th17 differentiation

Previous studies have demonstrated that CD28 signaling suppresses human Th17 differentiation through an AKT-dependent mechanism.[31] Our screen identified that CD28 and AKT1 may affect the function of pathogenic Th17 cells (Figures 3D and 3F), and the role of CD28 in the differentiation and function of pathogenic Th17 cells remains unclear. To address this, we performed both CRISPRi and CRISPRa systems in the process of Th17 differentiation (Figure 5A). Firstly, we employed CRISPRi-mediated gene silencing using multiple sgRNAs targeting *CD28* during *in vitro* differentiation of pathogenic Th17 cells. Intracellular cytokine staining was performed to assess the expression of IL-17A and GM-CSF on day 9 and day 16 after differentiation. Suppressing the expression of CD28 significantly increased the proportion of IL-17A$^+$CD4$^+$ T cells, IL-17A$^+$GM-CSF$^+$CD4$^+$ T cells, and IL-17A$^+$IFN-γ^+CD4$^+$ T cells (Figures 5B and 5D), whereas enhanced expression of CD28 via CRISPRa resulted in a marked decrease in these populations (Figures 5C and 5E), indicating that CD28 signaling negatively regulates pathogenic Th17 differentiation. To further validate the involvement of CD28 downstream signaling, we used AKTi VIII, a small molecule selectively inhibiting AKT1 and AKT2, key effectors of CD28-mediated signaling. AKTi VIII was continuously included throughout the Th17 differentiation process (Figure 5F). Consistent with the CRISPR-based findings, AKT inhibition led to a significant increase in the frequency of IL-17A$^+$CD4$^+$ T cells, IL-17A$^+$GM-CSF$^+$CD4$^+$, and IL-17A$^+$IFN-γ^+CD4$^+$ T cells (Figures 5G and 5H). Furthermore, qPCR analysis revealed that the expression of *CD28* was downregulated after AKTi and CRISPRi treatment, in contrast to its upregulation following CRISPRa treatment (Figures S8A–S8C). Together, these results demonstrate that CD28 signaling restricts the differentiation and functional maturation of pathogenic Th17 cells through an AKT-dependent pathway.

HMOX1 promotes the differentiation of pathogenic Th17 cells *in vitro*

HMOX1, a central enzyme in cellular antioxidant defense, plays a complex and critical role in the immune system.[36] It catalyzes the degradation of heme into carbon monoxide (CO), biliverdin/bilirubin, and free iron.[37] Recent studies have suggested that high HMOX1 expression has been associated with sustained inflammation and exacerbated pathological damage.[38,39] Furthermore, HMOX1 has been reported to regulate the Th17/Treg balance in murine models.[35] Our screen identified that HMOX1 may affect the function of pathogenic Th17 cells (Figures 3B and 3E), and its specific role in human pathogenic Th17 cell differentiation remains unclear. To address this, we first employed CRISPRi to suppress HMOX1 expression during *in vitro* differentiation of human Th17 cells (Figure 6A).

Intracellular cytokine staining on day 9 and day 16 after differentiation revealed that knockdown of HMOX1 led to a significant reduction in IL-17A production and a concomitant decrease in the frequency of both GM-CSF$^+$IL-17A$^+$CD4$^+$ and IL-17A$^+$IFN-γ^+CD4$^+$ T cells (Figures 6B and 6C), suggesting that HMOX1 positively regulates the differentiation of pathogenic Th17 cells. To further validate the role of HMOX1, we used pharmacologic modulators of HO-1 activity in the procedure of Th17 cell differentiation (Figure 6D). Hemin, a well-established inducer of HMOX1 and a substrate of HO-1, significantly increased HO-1 protein levels upon treatment.[40] In contrast, tin protoporphyrin IX (SNPP), a competitive inhibitor of HO-1, blocks its activity both *in vivo* and *in vitro*.[41,42] When Th17 cells were treated with hemin during differentiation, we observed a marked increase in the proportion of IL-17A$^+$GM-CSF$^+$ and IL-17A$^+$IFN-γ^+ Th17 cells. Conversely, treatment with SNPP resulted in a significant reduction in these populations (Figures 6E, 6F, S9A, and S9B). Furthermore, qPCR analysis revealed that the expression of *HMOX1* was upregulated after hemin treatment but downregulated after CRISPRi (Figures S8D and S8E).

To assess downstream iron-homeostasis responses associated with pharmacological modulation of HO-1, the expression of FTH1, *FTL*, and TFRC was examined. As expected, hemin treatment increased FTH1 and FTL mRNA expression, while reducing TFRC expression (Figures S10A–S10C). In contrast, SNPP decreased FTH1 and FTL expression and increased TFRC expression (Figures S10A–S10C). These results indicate that hemin and SNPP induced opposing changes in iron-homeostasis-related gene expression, consistent with activation and inhibition of HO-1-associated activity, respectively.

Collectively, these results demonstrate that HMOX1 facilitates the differentiation of human pathogenic Th17 cells *in vitro*. Genetic suppression of HMOX1 expression or pharmacological inhibition of HO-1-associated activity attenuated the emergence of IL-17A$^+$GM-CSF$^+$ Th17 cells, suggesting that HMOX1 may represent a potential therapeutic target in autoimmune and inflammatory disorders.

DISCUSSION

Pathogenic Th17 cells are recognized as key mediators of various autoimmune and inflammatory diseases. However, the critical regulatory genes controlling their differentiation and effector function remain incompletely defined, thereby hindering the development of targeted therapeutic strategies. In this study, we employed complementary CRISPRa and CRISPRi screens using customized druggable-gene libraries to systematically

(D and E) Flow cytometry analysis of IL-17A$^+$, IL-17A$^+$GM-CSF$^+$, and IL-17A$^+$IFN-γ^+ cells of the control and CRISPRi-CD28 sgRNA-transduced Th17 cells (D) and CRISPRa-CD28 sgRNA transduced Th17 cells (E) on day 16 after Th17 cell differentiation (n = 3).

(F) Scheme of AKTi treatment in the differentiation process.

(G and H) Similar to (D) and (E), flow cytometry analysis of IL-17A$^+$, IL-17A$^+$GM-CSF$^+$, and IL-17A$^+$IFN-γ^+ cells of the control and AKT-inhibitor treated Th17 cells (G) on day 9 and (H) day 16 after differentiation (n = 3). Data are presented as means ± SEM with statistical significance determined by ANOVA and unpaired t test. The normality of data was confirmed by Shapiro-Wilk test. Statistical significance was presented by $^*p < 0.05$, $^{**}p < 0.01$, and $^{***}p < 0.001$.

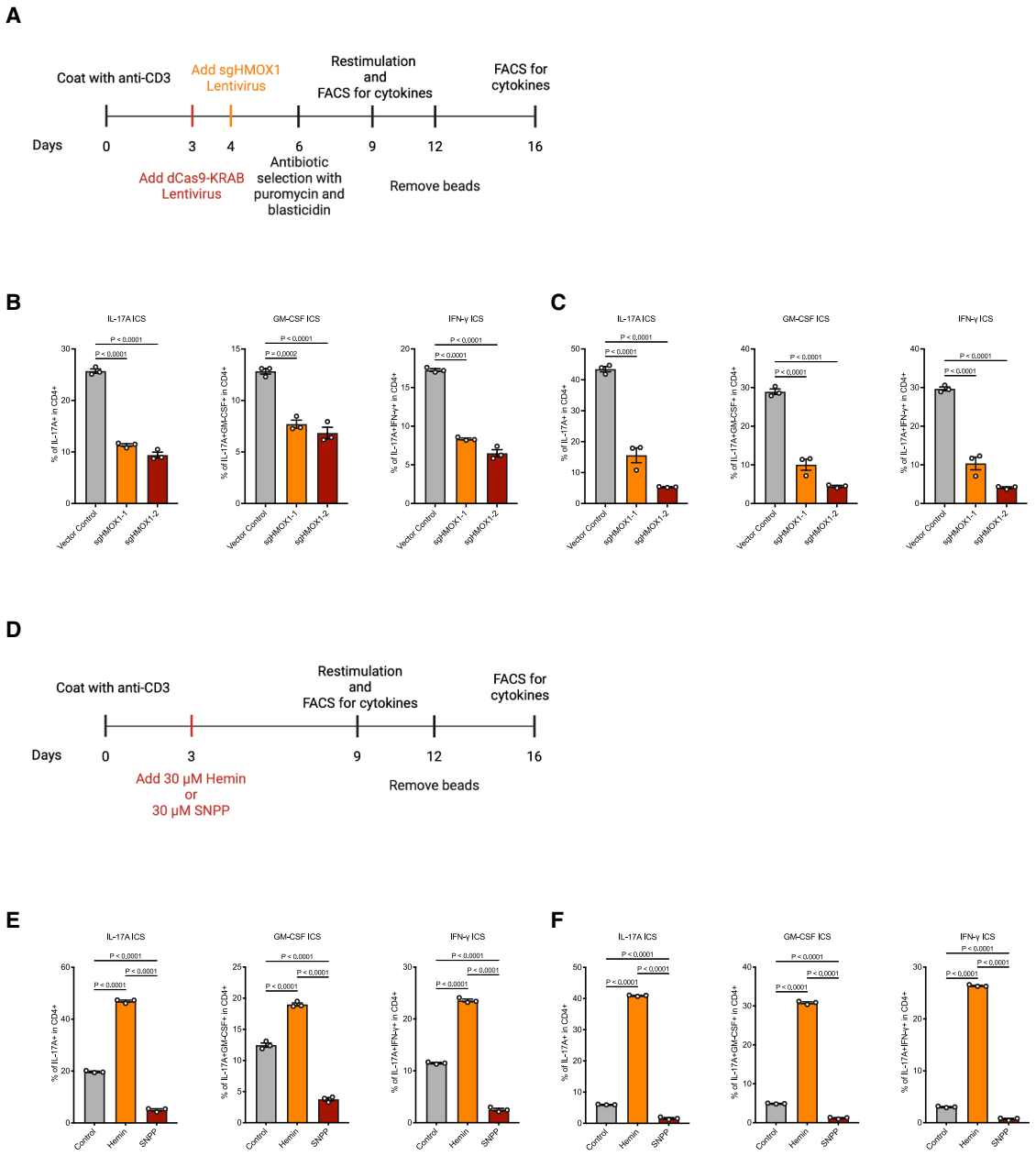


Figure 6. *HMOX1* promotes the differentiation of pathogenic Th17 cells *in vitro*

(A) Schematic diagram of Th17 cells treated with CRISPRi system targeting *HMOX1*.

(B and C) Flow cytometry analysis of IL-17A$^+$, IL-17A$^+$GM-CSF$^+$, and IL-17A$^+$IFN-γ$^+$ cells of the control and CRISPRi-HMOX1 sgRNA transduced Th17 cells on day 9 (B) or day 16 (C) after Th17 cell differentiation (n = 3).

(D) Scheme of hemin and SNPP treatment in the differentiation process.

(E and F) Flow cytometry analysis of IL-17A$^+$, IL-17A$^+$GM-CSF$^+$, and IL-17A$^+$IFN-γ$^+$ cells of the control and hemin- or SNPP-treated Th17 cells on day 9 (E) or day 16 (F) after Th17 cell differentiation (n = 3). See also Figures S9A and S9B. Data are presented as means ± SEM with statistical significance determined by ANOVA test. The normality of data was confirmed by Shapiro-Wilk test. Statistical significance was presented by $^*p < 0.05$, $^{**}p < 0.01$, and $^{***}p < 0.001$.

interrogate the genetic programs governing pathogenic human Th17 cell differentiation and activation. Our screens successfully identified several previously characterized regulators of Th17 cell function, including components of the CD28-AKT signaling pathway. Notably, HMOX1 emerged as a potential positive regulator, with HMOX1-targeting sgRNAs showing enrichment within the pathogenic Th17 population in the CRISPRa screen. Using individual sgRNAs, along with pharmacological modulators, we demonstrated that genetic suppression of HMOX1 expression or pharmacological inhibition of HO-1-associated activity reduced the differentiation and activation of pathogenic human Th17 cells. These findings suggest that targeting HMOX1 may

represent a promising strategy to mitigate Th17-driven autoimmune and inflammatory pathology. In addition to functional insights, our paired CRISPRa/i screen platform and customized sgRNA library provide a valuable resource for decoding the regulatory circuitry of pathogenic human Th17 cells.

Interestingly, while CD28—a well-established Th17 regulator—was robustly enriched in our screens, other known pathways such as RORγt[6], JAK-STAT,[43,44] and TGF-β[45,46] signaling were not significantly represented. One potential explanation is that the extended culture duration required for *in vitro* Th17 differentiation (9–16 days) may have masked the contributions of genes involved in cell survival or proliferation. To address this limitation, future studies could explore shortening the differentiation period or increasing the initial input of T cells to enhance screen sensitivity. Alternatively, the development of inducible CRISPRa/i systems may allow temporal control of gene perturbation and reduce selective pressure against essential genes, thereby improving the resolution of functional genetic screens in primary human T cells. Interestingly, CD28-targeting sgRNAs were enriched in IL-17A$^+$GM-CSF$^+$ double-positive cells even in the absence of added CD28 co-stimulation in our screen. We hypothesize that this may be due to endogenous CD28 ligands presented by macrophages and dendritic cells within the PBMC culture, which could exert a negative influence on the differentiation of pathogenic Th17 cells.

HMOX1 has been implicated in regulating the balance between Th17 and Treg cells in murine models.[35] In the DSS-induced colitis model, administration of hemin, an inducer of HMOX1 expression, ameliorated disease severity and was accompanied by a reduction in Th17 cells and an increase in Treg cells, whereas treatment with SNPP, a competitive inhibitor of HO-1, exacerbated inflammation.[35] *In vitro*, hemin suppressed Th17 differentiation while promoting Treg development under TGF-β-and IL-6-driven conditions; this effect was reversed by SNPP.[35] In contrast to these murine findings, our study revealed an opposite role for HMOX1 in human Th17 differentiation. Several factors may account for this discrepancy. A major consideration is the fundamental difference in the cytokine requirements and regulatory pathways governing Th17 differentiation between species. In mice, Th17 polarization is primarily driven by TGF-β and IL-6, and HMOX1 has been shown to interfere with IL-6 receptor signaling, thereby limiting Th17 development and favoring Treg induction. However, in humans, TGF-β and IL-6 alone induce minimal Th17 differentiation, and our own data support the dispensability of IL-6 in driving human Th17 lineage commitment *in vitro* (Figure 1B). Thus, the inhibitory effect of HMOX1 on IL-6R signaling may exert opposite consequences in human versus mouse systems due to differing dependencies on IL-6 signaling. We also tested Th17 differentiation using the murine "pathogenic" cytokine cocktail of TGF-β3 and IL-6,[17] but observed minimal induction efficiency in human T cells, further supporting the notion that distinct gene regulatory networks govern Th17 differentiation across species. These observations highlight the importance of dissecting species-specific mechanisms regulating Th17 cells, particularly in the context of developing targeted therapies for Th17-mediated autoimmune and inflammatory diseases. Given that the present study was conducted primarily *in vitro*, future studies will employ appropriate *in vivo* models, including adoptive transfer of genetically perturbed human Th17 cells into humanized mouse models of inflammation and autoimmunity, to determine whether these candidate regulators modulate pathogenic Th17 cell differentiation and function under pathological conditions.

In summary, our study presents a systematic and complementary CRISPRa/CRISPRi screening platform to identify regulatory genes controlling human pathogenic Th17 cell differentiation and activation. We identify HMOX1 as a positive regulator of pathogenic Th17 cells, with potential implications for modulating Th17-driven inflammation. These findings expand our understanding of human Th17 biology and offer a foundation for developing targeted therapeutic strategies against Th17-associated autoimmune and inflammatory diseases.

Limitations of the study

Several limitations of our study should be acknowledged. First, while we utilized the proinflammatory cytokines GM-CSF and IFN-γ as markers for pathogenic Th17 cells *in vitro*, their functional pathogenicity requires further validation using appropriate *in vivo* models. Second, the mechanistic basis of HMOX1 function in pathogenic Th17 cells remains to be fully elucidated. Although the opposing changes in *FTH1*, *FTL,* and *TFRC* expression following hemin and SNPP treatment were consistent with modulation of HO-1-associated activity, we did not directly measure HO-1 enzymatic activity or its heme catabolic products, such as biliverdin/bilirubin and carbon monoxide. Therefore, direct biochemical validation will be required in future studies to further confirm HO-1 activity and SNPP target engagement. In addition, future studies employing autoimmune disease models, such as EAE or colitis, to test the function of control versus HMOX1-inhibited Th17 cells *in vivo*, alongside comprehensive *in vitro* signaling and transcriptional analyses, will be essential to define the dynamic regulatory role of HMOX1 in pathogenic Th17 cell biology. Third, we observed a lower recovery rate of sgRNAs in the CRISPRa screen compared to CRISPRi, likely due to the technical challenges of efficient transcriptional activation in primary human T cells. Further optimization of the CRISPRa system, including vector design, promoter strength, and delivery methods, will be necessary to enhance the robustness of activation-based genetic screens in this context. Finally, due to resource constraints, we were unable to validate many of the interesting candidate genes identified on our screen. Future work will systematically validate these targets and dissect their regulatory roles in human pathogenic Th17 cells.

In addition, donor age, sex, and gender information were unavailable for the commercially obtained PBMCs. Therefore, potential sex- or gender-associated differences in pathogenic Th17 cell differentiation and responses to genetic perturbations could not be evaluated in this study.

RESOURCE AVAILABILITY

Lead contact

Further information and requests for resources and reagents should be directed to and will be fulfilled by the lead contact, Xuanming Yang (xuanmingyang@sjtu.edu.cn).

Materials availability

All unique/stable reagents generated in this study are available from the lead contact.

Data and code availability

- All relevant data supporting the findings of this study are included in the main text and Supplementary Information. The CRISPRa/CRISPRi screen sequencing data generated in this study have been deposited in the NCBI Sequence Read Archive (SRA) under BioProject accession PRJNA1541140 and SRA accession numbers (SRR41075446, SRR41075447, SRR41075448, SRR41075449, SRR41075450, SRR41075451) and are publicly available. The accession numbers are also listed in the key resources table. Other data reported in this paper can be obtained from the lead contact upon reasonable request.
- No custom code was used for the analysis of the results presented in this study.
- Any additional information required to reanalyze the data reported in this paper is available from the lead contact upon request.

ACKNOWLEDGMENTS

We would like to thank Dr. Haixia Jiang from the Core Facility and Technical Service Center for SLSB, School of Life Sciences and Biotechnology, Shanghai Jiao Tong University, for her assistance with cell sorting. X.Y. was supported by the National Natural Science Foundation of China (grant numbers 32470937 and 32261143731) and the Shanghai Jiao Tong University Scientific and Technological Innovation Funds (2019QYA11). This project is partially supported by Angel Pharmaceuticals Co., Ltd.

AUTHOR CONTRIBUTIONS

X.Y. conceptualized and designed the overall project. Y.W., Z.Y., L.W., J.Z., W.W., B. L., B. H., F.Z., L.Z., C.S., B.Z., K.L., and X.Y. performed the experiments and analyzed the data. X.Y., Z.Y., and Y.W. wrote the manuscript.

DECLARATION OF INTERESTS

Lixin Wang, Biao Zhou, and Kecheng Li are employees of Angel Pharmaceuticals Co., Ltd. All other authors declare no competing interests.

STAR★METHODS

Detailed methods are provided in the online version of this paper and include the following:

- KEY RESOURCES TABLE
- EXPERIMENTAL MODEL AND STUDY PARTICIPANT DETAILS
  - Source of primary human T cells
  - Cell line
  - Bacteria
- METHOD DETAILS
  - Isolation of human T cells
  - *In vitro* Th17 cell differentiation
  - Recombinant plasmids construction
  - Lentivirus production
  - Lentivirus infection
  - Intracellular cytokine staining
  - Transcription factor staining
  - Quantitative real-time PCR
  - CRISPRa and CRISPRi screens
  - CRISPR screen analysis
- QUANTIFICATION AND STATISTICAL ANALYSIS

SUPPLEMENTAL INFORMATION

Supplemental information can be found online at https://doi.org/10.1016/j.isci.2026.118180.

Received: December 4, 2025
Revised: April 10, 2026
Accepted: October 25, 2026

REFERENCES

1. Speiser, D.E., Chijioke, O., Schaeuble, K., and Münz, C. (2023). CD4+ T cells in cancer. Nat. Cancer *4*, 317–329. https://doi.org/10.1038/s43018-023-00521-2.
2. Dong, C. (2021). Cytokine Regulation and Function in T Cells. Annu. Rev. Immunol. *39*, 51–76. https://doi.org/10.1146/annurev-immunol-061020-053702.
3. Sun, L., Su, Y., Jiao, A., Wang, X., and Zhang, B. (2023). T cells in health and disease. Signal Transduct. Target. Ther. *8*, 235. https://doi.org/10.1038/s41392-023-01471-y.
4. Harrington, L.E., Hatton, R.D., Mangan, P.R., Turner, H., Murphy, T.L., Murphy, K.M., and Weaver, C.T. (2005). Interleukin 17-producing CD4+ effector T cells develop via a lineage distinct from the T helper type 1 and 2 lineages. Nat. Immunol. *6*, 1123–1132. https://doi.org/10.1038/ni1254.
5. Miossec, P., and Kolls, J.K. (2012). Targeting IL-17 and TH17 cells in chronic inflammation. Nat. Rev. Drug Discov. *11*, 763–776. https://doi.org/10.1038/nrd3794.
6. Ivanov, I.I., McKenzie, B.S., Zhou, L., Tadokoro, C.E., Lepelley, A., Lafaille, J.J., Cua, D.J., and Littman, D.R. (2006). The Orphan Nuclear Receptor RORγt Directs the Differentiation Program of Proinflammatory IL-17+ T Helper Cells. Cell *126*, 1121–1133. https://doi.org/10.1016/j.cell.2006.07.035.
7. Wacleche, V., Landay, A., Routy, J.P., and Ancuta, P. (2017). The Th17 Lineage: From Barrier Surfaces Homeostasis to Autoimmunity, Cancer, and HIV-1 Pathogenesis. Viruses *9*, 303. https://doi.org/10.3390/v9100303.
8. Wong, M.T., Ong, D.E.H., Lim, F.S.H., Teng, K.W.W., McGovern, N., Narayanan, S., Ho, W.Q., Cerny, D., Tan, H.K.K., Anicete, R., et al. (2016). A High-Dimensional Atlas of Human T Cell Diversity Reveals Tissue-Specific Trafficking and Cytokine Signatures. Immunity *45*, 442–456. https://doi.org/10.1016/j.immuni.2016.07.007.
9. Naik, S., Bouladoux, N., Wilhelm, C., Molloy, M.J., Salcedo, R., Kastenmuller, W., Deming, C., Quinones, M., Koo, L., Conlan, S., et al. (2012). Compartmentalized control of skin immunity by resident commensals. Science *337*, 1115–1119. https://doi.org/10.1126/science.1225152.
10. Bettelli, E., Korn, T., Oukka, M., and Kuchroo, V.K. (2008). Induction and effector functions of TH17 cells. Nature *453*, 1051–1057. https://doi.org/10.1038/nature07036.
11. Korn, T., Bettelli, E., Oukka, M., and Kuchroo, V.K. (2009). IL-17 and Th17 Cells. Annu. Rev. Immunol. *27*, 485–517. https://doi.org/10.1146/annurev.immunol.021908.132710.
12. Galluzzo, M., Talamonti, M., De Simone, C., D'Adamio, S., Moretta, G., Tambone, S., Caldarola, G., Fargnoli, M.C., Peris, K., and Bianchi, L. (2018). Secukinumab in moderate-to-severe plaque psoriasis: a multicenter, retrospective, real-life study up to 52 weeks observation. Expert Opin. Biol. Ther. *18*, 727–735. https://doi.org/10.1080/14712598.2018.1481503.
13. Kivelevitch, D.N., and Menter, A. (2015). Use of brodalumab for the treatment of psoriasis and psoriatic arthritis. Immunotherapy *7*, 323–333. https://doi.org/10.2217/imt.14.113.

14. Canavan, T.N., Elmets, C.A., Cantrell, W.L., Evans, J.M., and Elewski, B.E. (2016). Anti-IL-17 Medications Used in the Treatment of Plaque Psoriasis and Psoriatic Arthritis: A Comprehensive Review. Am. J. Clin. Dermatol. *17*, 33–47. https://doi.org/10.1007/s40257-015-0162-4.

15. Wendling, D., Verhoeven, F., and Prati, C. (2019). Anti-IL-17 monoclonal antibodies for the treatment of ankylosing spondylitis. Expert Opin. Biol. Ther. *19*, 55–64. https://doi.org/10.1080/14712598.2019.1554053.

16. Patra, A., Nayak, S., Moharana, A., Ojha, P., Das, S., Akhtar, J., Giri, B., and Singh, S. (2024). Preliminary Investigation and Therapeutic Efficacy Determination of a Novel Anti-IL-17A Antibody, Indikizumab. Biologics *18*, 257–271. https://doi.org/10.2147/BTT.S477752.

17. Lee, Y., Awasthi, A., Yosef, N., Quintana, F.J., Xiao, S., Peters, A., Wu, C., Kleinewietfeld, M., Kunder, S., Hafler, D.A., et al. (2012). Induction and molecular signature of pathogenic TH17 cells. Nat. Immunol. *13*, 991–999. https://doi.org/10.1038/ni.2416.

18. Yasuda, K., Takeuchi, Y., and Hirota, K. (2019). The pathogenicity of Th17 cells in autoimmune diseases. Semin. Immunopathol. *41*, 283–297. https://doi.org/10.1007/s00281-019-00733-8.

19. Achuthan, A.A., Lee, K.M.C., and Hamilton, J.A. (2021). Targeting GM-CSF in inflammatory and autoimmune disorders. Semin. Immunol. *54*, 101523. https://doi.org/10.1016/j.smim.2021.101523.

20. Cook, A.D., Louis, C., Robinson, M.J., Saleh, R., Sleeman, M.A., and Hamilton, J.A. (2016). Granulocyte macrophage colony-stimulating factor receptor alpha expression and its targeting in antigen-induced arthritis and inflammation. Arthritis Res. Ther. *18*, 287. https://doi.org/10.1186/s13075-016-1185-9.

21. Paré, A., Mailhot, B., Lévesque, S.A., Juzwik, C., Ignatius Arokia Doss, P.M., Lécuyer, M.A., Prat, A., Rangachari, M., Fournier, A., and Lacroix, S. (2018). IL-1beta enables CNS access to CCR2(hi) monocytes and the generation of pathogenic cells through GM-CSF released by CNS endothelial cells. Proc. Natl. Acad. Sci. USA *115*, E1194–E1203. https://doi.org/10.1073/pnas.1714948115.

22. Croxford, A.L., Lanzinger, M., Hartmann, F.J., Schreiner, B., Mair, F., Pelczar, P., Clausen, B.E., Jung, S., Greter, M., and Becher, B. (2015). The Cytokine GM-CSF Drives the Inflammatory Signature of CCR2+ Monocytes and Licenses Autoimmunity. Immunity *43*, 502–514. https://doi.org/10.1016/j.immuni.2015.08.010.

23. Ghoreschi, K., Laurence, A., Yang, X.P., Tato, C.M., McGeachy, M.J., Konkel, J.E., Ramos, H.L., Wei, L., Davidson, T.S., Bouladoux, N., et al. (2010). Generation of pathogenic T(H)17 cells in the absence of TGF-beta signalling. Nature *467*, 967–971. https://doi.org/10.1038/nature09447.

24. Shalem, O., Sanjana, N.E., Hartenian, E., Shi, X., Scott, D.A., Mikkelsen, T.S., Heckl, D., Ebert, B.L., Root, D.E., Doench, J.G., and Zhang, F. (2014). Genome-Scale CRISPR-Cas9 Knockout Screening in Human Cells. Science *343*, 84–87. https://doi.org/10.1126/science.1247005.

25. Tsujino, T., Takai, T., Hinohara, K., Gui, F., Tsutsumi, T., Bai, X., Miao, C., Feng, C., Gui, B., Sztupinszki, Z., et al. (2023). CRISPR screens reveal genetic determinants of PARP inhibitor sensitivity and resistance in prostate cancer. Nat. Commun. *14*, 252. https://doi.org/10.1038/s41467-023-35880-y.

26. Belk, J.A., Yao, W., Ly, N., Freitas, K.A., Chen, Y.T., Shi, Q., Valencia, A.M., Shifrut, E., Kale, N., Yost, K.E., et al. (2022). Genome-wide CRISPR screens of T cell exhaustion identify chromatin remodeling factors that limit T cell persistence. Cancer Cell *40*, 768–786.e7. https://doi.org/10.1016/j.ccell.2022.06.001.

27. Schmidt, R., Steinhart, Z., Layeghi, M., Freimer, J.W., Bueno, R., Nguyen, V.Q., Blaeschke, F., Ye, C.J., and Marson, A. (2022). CRISPR activation and interference screens decode stimulation responses in primary human T cells. Science *375*, eabj4008. https://doi.org/10.1126/science.abj4008.

28. Dominguez, A.A., Lim, W.A., and Qi, L.S. (2015). Beyond editing: repurposing CRISPR–Cas9 for precision genome regulation and interrogation. Nat. Rev. Mol. Cell Biol. *17*, 5–15. https://doi.org/10.1038/nrm.2015.2.

29. Mandegar, M.A., Huebsch, N., Frolov, E.B., Shin, E., Truong, A., Olvera, M.P., Chan, A.H., Miyaoka, Y., Holmes, K., Spencer, C.I., et al. (2016). CRISPR Interference Efficiently Induces Specific and Reversible Gene Silencing in Human iPSCs. Cell Stem Cell *18*, 541–553. https://doi.org/10.1016/j.stem.2016.01.022.

30. Manel, N., Unutmaz, D., and Littman, D.R. (2008). The differentiation of human T(H)-17 cells requires transforming growth factor-beta and induction of the nuclear receptor RORgammat. Nat. Immunol. *9*, 641–649. https://doi.org/10.1038/ni.1610.

31. Revu, S., Wu, J., Henkel, M., Rittenhouse, N., Menk, A., Delgoffe, G.M., Poholek, A.C., and McGeachy, M.J. (2018). IL-23 and IL-1beta Drive Human Th17 Cell Differentiation and Metabolic Reprogramming in Absence of CD28 Costimulation. Cell Rep. *22*, 2642–2653. https://doi.org/10.1016/j.celrep.2018.02.044.

32. Purvis, H.A., Stoop, J.N., Mann, J., Woods, S., Kozijn, A.E., Hambleton, S., Robinson, J.H., Isaacs, J.D., Anderson, A.E., and Hilkens, C.M.U. (2010). Low-strength T-cell activation promotes Th17 responses. Blood *116*, 4829–4837. https://doi.org/10.1182/blood-2010-03-272153.

33. Sanson, K.R., Hanna, R.E., Hegde, M., Donovan, K.F., Strand, C., Sullender, M.E., Vaimberg, E.W., Goodale, A., Root, D.E., Piccioni, F., and Doench, J.G. (2018). Optimized libraries for CRISPR-Cas9 genetic screens with multiple modalities. Nat. Commun. *9*, 5416. https://doi.org/10.1038/s41467-018-07901-8.

34. Chen, L., and Flies, D.B. (2013). Molecular mechanisms of T cell co-stimulation and co-inhibition. Nat. Rev. Immunol. *13*, 227–242. https://doi.org/10.1038/nri3405.

35. Zhang, L., Zhang, Y., Zhong, W., Di, C., Lin, X., and Xia, Z. (2014). Heme oxygenase-1 ameliorates dextran sulfate sodium-induced acute murine colitis by regulating Th17/Treg cell balance. J. Biol. Chem. *289*, 26847–26858. https://doi.org/10.1074/jbc.M114.590554.

36. Campbell, N.K., Fitzgerald, H.K., and Dunne, A. (2021). Regulation of inflammation by the antioxidant haem oxygenase 1. Nat. Rev. Immunol. *21*, 411–425. https://doi.org/10.1038/s41577-020-00491-x.

37. Liang, Z., Liu, J., Gou, Y., Wang, H., Li, Z., Cao, Y., Zhang, H., Bai, R., and Zhang, Z. (2025). Elevated Histone Lactylation Mediates Ferroptosis Resistance in Endometriosis Through the METTL3-Regulated HIF1A/HMOX1 Signaling Pathway. Adv. Sci. (Weinh). *12*, e08220. https://doi.org/10.1002/advs.202408220.

38. Schipper, H.M., Song, W., Tavitian, A., and Cressatti, M. (2019). The sinister face of heme oxygenase-1 in brain aging and disease. Prog. Neurobiol. (1956). *172*, 40–70. https://doi.org/10.1016/j.pneurobio.2018.06.008.

39. Wagener, F.A.D.T.G., Toonen, E.J.M., Wigman, L., Fransen, J., Creemers, M.C.W., Radstake, T.R.D.J., Coenen, M.J.H., Barrera, P., van Riel, P.L.C.M., and Russel, F.G.M. (2008). HMOX1 promoter polymorphism modulates the relationship between disease activity and joint damage in rheumatoid arthritis. Arthritis Rheum. *58*, 3388–3393. https://doi.org/10.1002/art.23970.

40. Vanova, K., Boukalova, S., Gbelcova, H., Muchova, L., Neuzil, J., Gurlich, R., Ruml, T., and Vitek, L. (2016). Heme oxygenase is not involved in the anti-proliferative effects of statins on pancreatic cancer cells. BMC Cancer *16*, 309. https://doi.org/10.1186/s12885-016-2343-9.

41. Abdalla, M.Y., Ahmad, I.M., Rachagani, S., Banerjee, K., Thompson, C.M., Maurer, H.C., Olive, K.P., Bailey, K.L., Britigan, B.E., and Kumar, S. (2019). Enhancing responsiveness of pancreatic cancer cells to gemcitabine treatment under hypoxia by heme oxygenase-1 inhibition. Transl. Res. *207*, 56–69. https://doi.org/10.1016/j.trsl.2018.12.008.

42. Tian, J., Li, Y., Mao, X., Xie, K., Zheng, Y., Yu, Y., and Yu, Y. (2023). Effects of the PI3K/Akt/HO-1 pathway on autophagy in a sepsis-induced acute lung injury mouse model. Int. Immunopharmacol. *124*, 111063. https://doi.org/10.1016/j.intimp.2023.111063.

43. Wang, F., Yang, Y., Li, Z., Wang, Y., Zhang, Z., Zhang, W., Mu, Y., Yang, J., Yu, L., and Wang, M. (2022). Mannan-Binding Lectin Regulates the Th17/Treg Axis Through JAK/STAT and TGF-β/SMAD Signaling Against Candida albicans Infection. J. Inflamm. Res. *15*, 1797–1810. https://doi.org/10.2147/jir.S344489.

44. Fan, X., Xu, M., Wang, Z., Sun, X., Fan, Y., Chen, J., Hao, J., Wang, R., and Jia, W. (2025). Arctiin suppress Th17 cells response and ameliorates experimental autoimmune uveitis through JAK/STAT signaling. Cell. Immunol. *409–410*, 104927. https://doi.org/10.1016/j.cellimm.2025.104927.

45. Wang, J., Zhao, X., and Wan, Y.Y. (2023). Intricacies of TGF-beta signaling in Treg and Th17 cell biology. Cell. Mol. Immunol. *20*, 1002–1022. https://doi.org/10.1038/s41423-023-01036-7.

46. Wu, B., Zhang, S., Guo, Z., Bi, Y., Zhou, M., Li, P., Seyedsadr, M., Xu, X., Li, J.L., Markovic-Plese, S., and Wan, Y.Y. (2021). The TGF-beta superfamily cytokine Activin-A is induced during autoimmune neuroinflammation and drives pathogenic Th17 cell differentiation. Immunity *54*, 308–323.e6. https://doi.org/10.1016/j.immuni.2020.12.010.

STAR★METHODS

KEY RESOURCES TABLE

REAGENT or RESOURCE	SOURCE	IDENTIFIER
Antibodies		
anti-hCD4 BV711	BD Biosciences	Cat# 563028; RRID: AB_2737961
anti-IL-17A PE	Invitrogen	Cat# 12–7178-42; RRID: AB_1272095
anti-GM-CSF APC	Biolegend	Cat# 502310; RRID: AB_11150231
anti-IFN-γ PE-Cy7	Biolegend	Cat# 502529; RRID: AB_10663411
anti-hCD4 BV421	Biolegend	Cat# 344632; RRID: AB_2566015
anti-T-bet FITC	Biolegend	Cat# 644812; RRID: AB_2200540
anti-AhR PE-CF594	BD Biosciences	Cat# 565790; RRID: AB_2869714
anti-RORγt PE	Invitrogen	Cat# 12–6988-82; RRID: AB_1834470
anti-FOXP3 AF647	Biolegend	Cat# 320014; RRID: AB_439750
Bacterial and virus strains		
E. coli Trans1-T1 (phage resistant)	TransGen Biotech	Cat# CD501-02
Biological samples		
Human peripheral blood mononuclear cells	Milecell Bio	Cat# PB010C, Lot# P122060502C
Human peripheral blood mononuclear cells	Milecell Bio	Cat# PB025C-W Lot# P122041602C
Human peripheral blood mononuclear cells	Milecell Bio	Cat# PB010C Lot# P122020711C
Human peripheral blood mononuclear cells	Milecell Bio	Cat# PB010C Lot# P122120704C
Chemicals, peptides, and recombinant proteins		
anti-human-IL4	Biolegend	Cat# 500838; RRID: AB_2810616
anti-human-IFN-γ	Biolegend	Cat# 506532; RRID: AB_2801092
human IL-2	Beijing Four Rings Bio-Pharma	National Drug Approval Number:S10970017
human IL-23	Sino Biological	Cat# CT012-H08H
human IL-1β	Sino Biological	Cat# 10139-HNAE
human TGF-β1	Novoprotein	Cat# CA59
human TGF-β3	YEASEN	Cat# GMP-TC646-0050
human IL-6	Sino Biological	Cat# 10395-HNAE
AKTi	TargetMol	Cat# T3346
Hemin	MedChemExpress	Cat# HY19424
SNPP	MedChemExpress	Cat# HY101194
NaOH	BBILife Science	Cat# A620617
ViralBoost Reagent	Alstem Bio	Cat# BV100
Lentiviral Concentrator	TAKARA	Cat# 631232
Sodium Pyruvate	Gibco	Cat# 11360070
Nonessential amino acids	Gibco	Cat# 11140050
Penicillin/Streptomycin	Meilun Bio	Cat# MA0110
β-mercaptoethanol	Gibco	Cat# 31350010
RPMI 1640	Gibco	Cat# C11875500BT
X-VIVO™ 15	Lonza	Cat# 04-418Q
UniEx™	Excell Bio	Cat# TE000-N021
Blasticidin	Invivogen	Cat# ant-bl-05
Puromycin	Invivogen	Cat# ant-pr-1

(*Continued on next page*)

Continued

REAGENT or RESOURCE	SOURCE	IDENTIFIER
FBS	Gibco	Cat# 10010023
L-Glutamine	Gibco	Cat# 21051040
OPTI-MEM	Gibco	Cat# 32985070
αCD3/CD28 beads	Invitrogen	Cat# 1132D; RRID: AB_2943359
anti-CD3	Bio X cell	Cat# BE0001-2; RRID: AB_1107632
PBS	Gibco	Cat# C10010500BT
TRIzol reagent	Invitrogen	Cat# 15596018CN
Brefeldin A	Biolegend	Cat# 420601
Cell Stimulation cocktail	Invitrogen	Cat# 00–4970-93
ChamQ Universal qPCR SYBR Green Master Mix	Vazyme Labs	Cat# Q711-02
Critical commercial assays		
Lipofectamine 3000 Transfection Kit	Invitrogen	Cat# L3000-015
NucleoBond Xtra Midi	MACHEREY-NAGEL	Cat# 740410.50
Intracellular Fixation & Permeabilization Buffer Set	Invitrogen	Cat# 88–8824-00
FOXP3/Transcription Factor Staining Buffer Set	Invitrogen	Cat# 00–5523-00
Total RNA Kit I	Omega Bio-Tek	Cat# R6834-01
Tissue DNA Kit	Omega Bio-Tek	Cat# D3396-00
GoScript Reverse Transcription System	Promega	Cat# A5001
MycoBlue Mycoplasma Detector	Vazyme	Cat# D101-01
Deposited data		
CRISPRa/CRISPRi screen sequencing data	NCBI Sequence Read Archive	BioProject: PRJNA1541140 SRA: SRR41075446, SRR41075447, SRR41075448, SRR41075449 SRR41075450, SRR41075451
Experimental models: Cell lines		
Lenti-X 293T	Clontech	Cat# 632180 RRID:CVCL_4401
Oligonucleotides		
sgRNA target HMOX1 (CRISPRi)-1 sequence: 5′-CGCGGGCGGCGGCTGCGCTG-3′	This paper	N/A
sgRNA target HMOX1 (CRISPRi)-2 sequence: 5′- CGAACGAGCCCAGCACCGGC-3′	This paper	N/A
sgRNA target CD28 (CRISPRa)-1 sequence: 5′-CCTTGATCATGTGCCCTAAG-3′	This paper	N/A
sgRNA target CD28 (CRISPRa)-2 sequence: 5′-ATCAAGGCACTCAAACCACA-3′	This paper	N/A
sgRNA target CD28 (CRISPRi)-1 sequence: 5′-TCGTCAGGACAAAGATGCTC-3′	This paper	N/A
sgRNA target CD28 (CRISPRi)-2 sequence: 5′-GAGCATCTTTGTCCTGACGA-3′	This paper	N/A
Recombinant DNA		
pXPR_502-sgRNA expression backbone	Addgene	Cat# 96923
pXPR_050-sgRNA expression backbone	Addgene	Cat# 96925
pMSCV-dCas9-VP64	This paper	N/A
pMSCV-dCas9-KRAB	This paper	N/A
pMD2.G	Addgene	Cat# 12259
psPAX2	Addgene	Cat# 12260
Software and algorithms		
Graphpad Prism 10.2.0	Dotmatics	https://www.graphpad.com/
FlowJo version 10	BD Biosciences	https://www.flowjo.com/
MAGeCK 0.5.9.6	MAGeCK developers	https://sourceforge.net/p/mageck/wiki/Home/

(*Continued on next page*)

Continued

REAGENT or RESOURCE	SOURCE	IDENTIFIER
Other		
FACS Aria III	BD Biosciences	N/A
FACS CytoFLEX S flow cytometer	Beckman Coulter	N/A

EXPERIMENTAL MODEL AND STUDY PARTICIPANT DETAILS

Source of primary human T cells

Human peripheral blood mononuclear cells (PBMCs) from healthy donors were collected from healthy volunteers following informed consent and commercially sourced through Milecell Biotechnology (Shanghai, China). Donor age, sex, and gender information was not available to the investigators.

Cell line

Lenti-X 293T cells (Clontech, #632180), originating from female fetal tissue, were cultured in DMEM supplemented with 10% FBS and 100 U/mL penicillin-streptomycin in a 37 °C incubator with 5% CO_2. The cell line was not independently authenticated in our laboratory. Mycoplasma contamination was assessed using MycoBlue Mycoplasma Detector (Vazyme, #D101-01), and the results were negative.

Bacteria

Trans1-T1 phage-resistant chemically competent *Escherichia coli* cells (TransGen Biotech, #CD501-02; genotype: F^- φ80(*lacZ*)ΔM15 Δ*lacX74 hsdR*(r_K^-, m_K^+) Δ*recA1398 endA1 tonA*) were used for molecular cloning. The bacteria were cultured in LB broth supplemented with a selection antibiotic at 37 °C in a shaker set to 300 rpm or on LB-agar plates supplemented with a selection antibiotic at 37 °C in a plate incubator.

METHOD DETAILS

Isolation of human T cells

Naive $CD4^+$ cells were isolated from PBMCs by negative selection using the Human Naive $CD4^+$ T cell Isolation Kit II (Immunosep). Isolated cells were assessed for purity by flow cytometry. Cell purity exceeded 95% in most donor batches. Purified $CD4^+$ T cells were cultured in multiple conditions for differentiation of Th17 cells.

In vitro Th17 cell differentiation

Primary T cells were activated with 5 μg/mL plate-bound human anti-CD3 (Bio X Cell, #BE0001-2) or anti-human CD3/CD28 beads (Invitrogen, #1132D) at multiple cell-to-bead ratios. For screening, X-VIVO 15 (Lonza, #04-418Q), UniEx (Excell, #TE000-N021), and RPMI 1640 (Gibco, #C11875500BT) medium were used. For finalized Th17 cell differentiation, unless stated otherwise, cells were cultured initially in complete RPMI medium supplemented with 9% heat-inactivated fetal bovine serum (FBS, Gibco #10010023), 2 mM L-glutamine (Gibco, #21051040), 100 U/mL penicillin/streptomycin (Meilun Bio, #MA0110), 55 μM β-mercaptoethanol (Gibco, #31350010) and 10 IU/mL recombinant human (rh) IL-2 (Beijing Four Rings Bio-Pharma, #S10970017), 20 ng/mL IL-1β (Sino Biological, #10139-HNAE), 20 ng/mL rhIL-23 (Sino biological, #CT012-H08H), 1 ng/mL TGF-β1 (Novoprotein, #CA59), 5 μg/mL anti-IL-4 (Biolegend, #500838), 5 μg/mL anti-IFN-γ (Biolegend, #506532). Three days after activation, live T cells were enriched through Ficoll-paque density gradient centrifugation. T cells were maintained in Th17 culture medium described above with medium changed every two days. After 9 days of culture, Th17 cells were restimulated with anti-CD3/CD28 beads (Invitrogen, #1132D) at a cell-to-bead ratio of 1:4 (equivalent to 0.625 μL per 10^5 cells). Three days later, beads were removed using a magnetic stand. On day 16 after Th17 cell differentiation, cells were collected for intracellular cytokine staining, transcription factor staining, and sorting.

Recombinant plasmids construction

The dCas9-VP64-blasticidin insert was cloned from lenti dCas9-VP64-Blast (Addgene, Cat# 61425), and subsequently cloned into pMSCV lentiviral vector to generate pMSCV-dCas9-VP64-Blasticidin. The dCas9 and KRAB inserts were cloned from pZR071_SFFV-dCas9-mCherry-KRAB (Addgene, Cat# 180264) and then linked to the blasticidin resistant genes with T2A peptide sequence by overlap PCR to generate dCas9-KRAB-Blasticidin insert. This sequence was also cloned into pMSCV lentiviral vector to generate pMSCV-dCas9-KRAB-Blasticidin plasmid.

The sgRNA sequences for our druggable gene library were derived from the Sanson et al. Calabrese (CRISPRa) and Dolcetto (CRISPRi) whole-genome libraries (Data S1 and S2). The CRISPRi sgRNAs were effective near the transcription start site (TSS),

about +25 to +75 nt downstream of the TSS. In contrast, the CRISPRa sgRNAs targeted a region which was −150 to −75 nt upstream of the TSS. Individual sgRNA oligonucleotides for functional experiments were synthesized by Genewiz with BsmBI restriction endonuclease sites. Then the oligomers were annealed and cloned into the digested pXPR_502 (Addgene, #96923) for CRISPRa and pXPR_050 (Addgene, #96925) for CRISPRi. The library plasmids were obtained in large quantities using the NucleoBond Xtra Midi kit.

Lentivirus production

Lentivirus was produced by transient transfection of Lenti-X 293T cells (Clontech, #632180) using a second-generation lentiviral packaging system. One day before transfection, Lenti-X 293T cells were seeded in 293 medium X, OPTI-MEM (Gibco, #32985070) with 1 mM sodium pyruvate (Gibco, #11360070), 1× nonessential amino acids (Gibco, #11140050) and 5% FBS, at a density of 9.7×10^6 cells per 100 mm dish. Cells were incubated overnight in a 37 °C incubator with 5% CO_2. The following morning, cells at 85–95% confluency were co-transfected with 10.58 μg of lentiviral transfer plasmid, 7.56 μg of psPAX2 (Addgene, #12260), and 3.27 μg of pMD2.G (Addgene, #12259) per 100 mm dish. Transfection was performed using lipofectamine 3000 transfection kit (Invitrogen, #L3000-015) according to the manufacturer's protocol. Six hours post-transfection, the medium was replaced with fresh medium supplemented with 1× ViralBoost (Alstem Bio., #BV100). Lentiviral supernatant was harvested 24 h and 48 h after transfection. The two collections were pooled and filtered through 0.45 μm pore-size filter. The clarified supernatant was concentrated with Lenti-X-Concentrator (Takara Bio, #631232) according to the manufacturer's protocol. Lentiviral particles were resuspended in OPTI-MEM (Gibco, #32985070) at 1/100 of the original volume, then aliquoted, and frozen at −80°C until use.

Lentivirus infection

Primary T cells were activated and differentiated as described in "*In vitro* Th17 cell differentiation" section. For lentiviral infection, Th17 cells were infected with CRISPRa and CRISPRi tool lentiviruses encoding dCas9-VP64-Blasticidin or dCas9-KRAB-Blasticidin on day 3 after activation, and sgRNA library lentiviruses on day 4 after activation. Transduced Th17 cells were selected with 2.5 μg/mL blasticidin (Invivogen, #ant-bl-05) and 0.125 μg/mL puromycin (Invivogen, #ant-pr-1) from day 6 after activation.

Intracellular cytokine staining

After differentiation, Th17 cells were cultured at 1.5×10^6 cells/mL and restimulated with CD3/CD28 beads (Invitrogen, #1132D) at a cell-to-bead ratio of 1:4 (equivalent to 0.625 μL per 10^5 cells). Eighteen hours later, Brefeldin A (1:1000 dilution, Biolegend, #420601) and cell stimulation cocktails (1:500 dilution, Invitrogen, #00–4970-93) were added. Five hours later, cells were fixed and permeabilized with Intracellular Fixation and Permeabilization Buffer Set (Invitrogen, #88–8824-00) according to the manufacturer's protocol. Then staining for surface and intracellular markers was performed simultaneously with antibodies: anti-CD4 BV711 (BD Bioscience, #563028) or anti-CD4 BV421 (Biolegend, #344632), anti-IL-17A PE (Invitrogen, #12–7178-42), anti-GM-CSF APC (Biolegend, #502310), and anti-IFN-γ PE-Cy7 (Biolegend #502529), were used to stain Th17 cells in 1 × Permeabilization Buffer for 30 min at room temperature. Cells were washed with 1 × Permeabilization Buffer and resuspended in PBS containing 2% FBS for flow cytometric analysis. FACS Aria III sorter (BD Biosciences) was used for sorting. The CytoFLEX S flow cytometry (Beckman Coulter) was used for flow cytometry analysis. The FACS data were analyzed by FlowJo software (Tree Star). The universal gating strategy used for all flow-cytometric analysis is shown in Figure S1.

Transcription factor staining

After differentiation for 9 days or 16 days, Th17 cells were harvested for transcription factor staining. Cells were fixed and permeabilized using FOXP3/Transcription Factor Staining Buffer Set (Invitrogen, #00–5523-00) according to the manufacturer's protocol. Then the surface and transcription factor staining were performed simultaneously with antibodies: anti-CD4 BV421 (Biolegend, #344632), anti-T-bet FITC (Biolegend, #644812), anti-AhR PE-CF594 (BD Biosciences, #565790), anti-RORγt PE (Invitrogen, #12–6988-82), and anti-FOXP3 AF647 (Biolegend, #320014) in 1 × wash buffer for 30 min in 4 °C. Cells were washed with 1 × wash buffer and resuspended in PBS containing 2% FBS for flow cytometric analysis. The CytoFLEX S flow cytometer (Beckman Coulter) was used for flow cytometry analysis. The FACS data were analyzed by FlowJo software (Tree Star).

Quantitative real-time PCR

Total RNA from culture cells was extracted using a Total RNA Kit (Omega Bio-tek, #R6834-01) and reverse transcribed into cDNA using the GoScript Reverse Transcription System (Promega, #A5001). Quantitative PCR reactions were performed in triplicate using ChamQ Universal qPCR SYBR Green Master mix (Vazyme, #Q711-02). A melting-curve analysis was performed after amplification to verify the specificity of the PCR products. GAPDH was used as the endogenous reference gene. The relative quantification of the products was calculated by the $2^{-\Delta\Delta Ct}$ method. The primers for *GAPDH* (F: GGAGCGAGATCCCTCCAAAAT; R: GGCTGTTGTCATACTTCTCATGG), *CD28* (F: CTATTTCCCGGACCTTCTAAGCC; R: GCGGGGAGTCATGTTCATGTA), *HMOX1* (F: AAGACTGCGTTCCTGCTCAAC; R: AAAGCCCTACAGCAACTGTCG), *FTH1* (F: TGAAGCTGCAGAACCAACGAGG; R: GCACACTCCATTGCATTCAGCC), *FTL* (F: TACGAGCGTCTCCTGAAGATGC; R: GGTTCAGCTTTTTCTCCAGGGC), *TFRC* (F: ATCGGTTGGTGCCACTGAATGG; R: ACAACAGTGGGCTGGCAGAAAC) were obtained from Genewiz.

CRISPRa and CRISPRi screens

A total of 1×10^7 primary T cells were used as the starting population and infected with sgRNA library lentiviruses at an MOI of roughly 0.5. After intracellular cytokine staining of CRISPRa or CRISPRi library-transduced Th17 cells, the $CD4^+$ T cells were sorted into four subgroups, IL-17A$^+$GM-CSF$^+$, IL-17A$^+$GM-CSF$^-$, IL-17A$^-$GM-CSF$^+$, and IL-17A$^-$GM-CSF$^-$. Approximately 1–2 $\times$ 10^6 cells were sorted per group for sequencing. Genomic DNA was extracted from sorted cells using Tissue DNA Kit (Omega, #D3396-00). The integrated sgRNA sequences were amplified and purified by agarose gel electrophoresis. The purified libraries were sequenced on a NextSeq500 platform by Genewiz, and the resulting sequencing data were analyzed as described below.

CRISPR screen analysis

Reads were aligned to the appropriate reference library using MAGeCK version 0.5.9.6. The staggered 5′ adapter was automatically removed. The raw read counts of different groups were selected to remove all-zero sgRNAs. The cleaned read counts in IL-17A$^+$GM-CSF$^+$ versus IL-17A$^-$GM-CSF$^-$ were compared using mageck test with *-norm-method total* options. Gene hits were regarded as having a log2-fold change >0.5 and a -$\log_{10}$ (*p* value) > 1.3. The gene hits were then enriched by GO enrichment or KEGG enrichment to annotate the function and the involved pathway of the hits.

QUANTIFICATION AND STATISTICAL ANALYSIS

The statistical analyses of sequencing data were performed in R version 4.3.2. The other statistics were performed using GraphPad Prism 10.2.0 (GraphPad Software). Statistical significance was assessed using one-way analysis of variance (ANOVA) followed by Tukey's or Dunnett's multiple-comparisons test for comparisons among three or more groups and a two-tailed unpaired Student's *t* test for comparisons between two independent groups. Normality was assessed using the Shapiro–Wilk test, with a *p* value >0.05 indicating no significant deviation from normality. Statistical significance was presented by $^*p < 0.05$, $^{**}p < 0.01$, and $^{***}p < 0.001$.